

Inference of Tumor Evolution during Chemotherapy by Computational Modeling and In Situ Analysis of Genetic and Phenotypic Cellular Diversity

Vanessa Almendro,^{1,2,3,4} Yu-Kang Cheng,^{5,6} Amanda Randles,^{5,6,7} Shalev Itzkovitz,^{8,9} Andriy Marusyk,^{1,2,3} Elisabet Ametller,⁴ Xavier Gonzalez-Farre,⁴ Montse Muñoz,⁴ Hege G. Russnes,^{10,11,12} Åslaug Helland,^{10,13,14} Inga H. Rye,^{10,11} Anne-Lise Borresen-Dale,^{10,11} Reo Maruyama,^{1,2,3} Alexander van Oudenaarden,^{8,15} Mitchell Dowsett,¹⁶ Robin L. Jones,^{16,17} Jorge Reis-Filho,^{16,18} Pere Gascon,⁴ Mithat Gönen,¹⁹ Franziska Michor,^{5,6,*} and Kornelia Polyak^{1,2,3,20,21,*}

¹Department of Medical Oncology, Dana-Farber Cancer Institute, Boston, MA 02215, USA

²Department of Medicine, Brigham and Women's Hospital, Boston, MA 02115, USA

³Department of Medicine, Harvard Medical School, Boston, MA 02115, USA

⁴Department of Medical Oncology, Hospital Clinic, Institut d'Investigacions Biomediques August Pi i Sunyer, Barcelona 08036, Spain

⁵Department of Biostatistics and Computational Biology, Dana-Farber Cancer Institute, Boston, MA 02215, USA

⁶Department of Biostatistics, Harvard School of Public Health, Boston, MA 02115, USA

⁷Center for Applied Scientific Computing, Lawrence Livermore National Laboratory, Livermore, CA 94550, USA

⁸Departments of Physics and Biology and Koch Institute for Integrative Cancer Research, Massachusetts Institute of Technology, Cambridge, MA 02139, USA

⁹Department of Molecular Cell Biology, Weizmann Institute of Science, Rehovot 76100, Israel

¹⁰Department of Genetics, Institute for Cancer Research, Oslo University Hospital Radiumhospitalet, Oslo 0424, Norway

¹¹K.G. Jebsen Center for Breast Cancer Research, Institute for Clinical Medicine, Faculty of Medicine, University of Oslo, Oslo 0316, Norway

¹²Department of Pathology, Oslo University Hospital, Oslo 0424, Norway

¹³Department of Oncology, Oslo University Hospital, Oslo 0424, Norway

¹⁴Institute for Clinical Medicine, Faculty of Medicine, University of Oslo, Oslo 0316, Norway

¹⁵Hubrecht Institute, Royal Netherlands Academy of Arts and Sciences and University Medical Center Utrecht, Uppsalaalaan 8, 3584 CT, Utrecht, the Netherlands

¹⁶The Royal Marsden Hospital, The Breakthrough Breast Cancer Research Centre, Institute of Cancer Research, London SW3 6JJ, UK

¹⁷Seattle Cancer Care Alliance, Seattle, WA 98109-1023, USA

¹⁸Department of Pathology, Memorial Sloan-Kettering Cancer Center, New York, NY 10065, USA

¹⁹Department of Epidemiology and Biostatistics, Memorial Sloan-Kettering Cancer Center, New York, NY 10065, USA

²⁰Harvard Stem Cell Institute, Cambridge, MA 02138, USA

²¹Broad Institute, Cambridge, MA 02142, USA

*Correspondence: michor@jimmy.harvard.edu (F.M.), kornelia_polyak@dfci.harvard.edu (K.P.)

<http://dx.doi.org/10.1016/j.celrep.2013.12.041>

This is an open-access article distributed under the terms of the Creative Commons Attribution-NonCommercial-No Derivative Works License, which permits non-commercial use, distribution, and reproduction in any medium, provided the original author and source are credited.

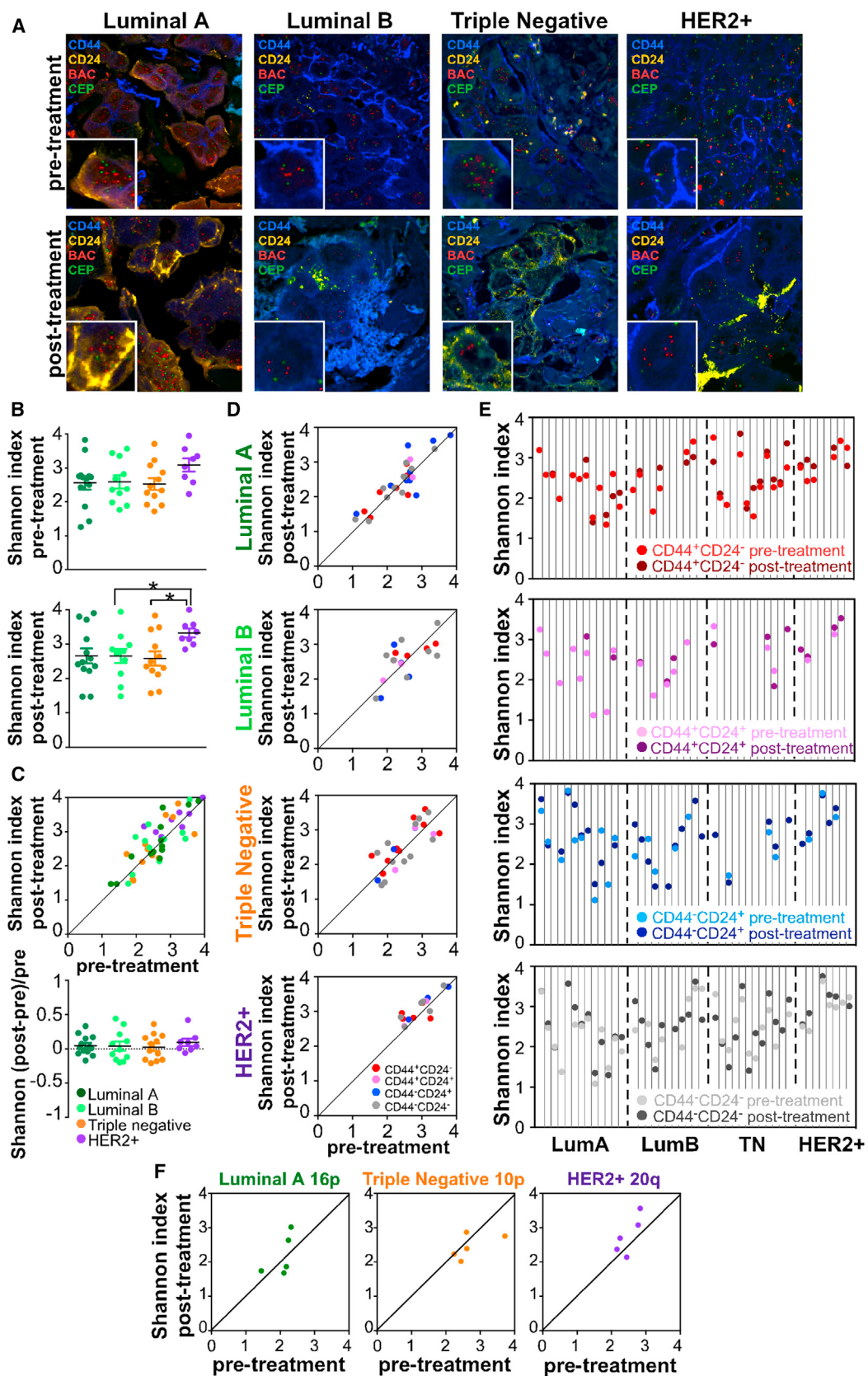
SUMMARY

Cancer therapy exerts a strong selection pressure that shapes tumor evolution, yet our knowledge of how tumors change during treatment is limited. Here, we report the analysis of cellular heterogeneity for genetic and phenotypic features and their spatial distribution in breast tumors pre- and post-neoadjuvant chemotherapy. We found that intratumor genetic diversity was tumor-subtype specific, and it did not change during treatment in tumors with partial or no response. However, lower pretreatment genetic diversity was significantly associated with pathologic complete response. In contrast, phenotypic diversity was different between pre- and post-treatment samples. We also observed significant changes in the spatial distribution of cells with

distinct genetic and phenotypic features. We used these experimental data to develop a stochastic computational model to infer tumor growth patterns and evolutionary dynamics. Our results highlight the importance of integrated analysis of genotypes and phenotypes of single cells in intact tissues to predict tumor evolution.

INTRODUCTION

Intratumor phenotypic heterogeneity is a defining characteristic of human tumors. Cancer cells within a tumor can display differences in many measurable traits, such as proliferative and metastatic capacity and therapeutic resistance (Almendro et al., 2013; Fidler, 1978; Heppner and Miller, 1983; Maley et al., 2006; Marusyk et al., 2012; Yap et al., 2012). Multiple mechanisms underlie intratumor heterogeneity, including both



heritable and nonheritable determinants (Fidler, 1978; Heppner and Miller, 1983; Maley et al., 2006; Marusyk et al., 2012; Marusyk and Polyak, 2010; Yap et al., 2012). In addition, cellular genetic diversity was observed within populations of tumor cells that is distinct from clonal diversity because it combines inputs from both clonal architecture and lower-scale differences arising from genomic instability that are not amplified by selection (Maley et al., 2006; Merlo et al., 2006). The study and treatment of cancer are complicated by this heterogeneity because small tissue samples, typically obtained by biopsy, may not be representative of the whole tumor (Gerlinger et al., 2012), and a treatment that targets one tumor cell population may not be effective against another (Turner and Reis-Filho, 2012; Yap et al., 2012).

Quantitative measures of intratumor heterogeneity might aid in the clinical management of patients with cancer including identifying those at a high risk of progression and recurrence. For example, a larger extent of intratumor clonal heterogeneity is associated with a higher risk of invasive progression in Barrett's esophagus (Maley et al., 2006; Merlo et al., 2010), and higher genetic heterogeneity in head and neck squamous carcinomas is related to worse outcome (Mroz et al., 2013). The presence of multiple cellular clones with distinct genetic alterations has also been implicated in therapeutic resistance (Engelman et al., 2007; Mroz et al., 2013; Nazarian et al., 2010; Sakai et al., 2008) and in metastatic progression (Fidler, 1978).

Cancer therapy exerts a strong selection pressure that shapes tumor evolution (Merlo et al., 2006). Thus, residual tumors after treatment are likely to have different, frequently less-favorable characteristics and composition than those of the diagnostic sample. Despite the importance of these treatment-induced changes for the success of subsequent therapy, tumors have been rarely resampled and reanalyzed, with the exception of hematopoietic malignancies (Ding et al., 2012; Landau et al., 2013). Thus, our understanding of how treatment impacts intratumor heterogeneity and cellular diversity in solid tumors, which then in turn determines the effectiveness of treatment, is very limited.

The most informative approach to uncover intratumor heterogeneity in clinical samples is the definition of the overall clonal architecture within a tumor. However, this level of resolution is not practically feasible. A lower-resolution view of clonal architecture can be outlined based on computational inferences from allele frequencies of whole-genome sequencing of bulk tumors (Ding et al., 2012) or by low-resolution sequencing of single cancer cells (Navin et al., 2011). Unfortunately, both of these approaches have many technical caveats and are prohibitively expensive to apply for large patient cohorts.

An alternative to the whole-genome studies is to study genetic diversity using a single or a few genomic loci. Although this approach cannot reveal the clonal architecture within a tumor, it is more feasible due to minimal sample requirements and low cost. Importantly, diversity indices calculated based on a limited number of loci (even selectively neutral ones) have been shown to predict clinical outcome (Maley et al., 2006; Merlo et al., 2010). Cellular heterogeneity reflects both clonal heterogeneity and genetic instability; thus, it can be impacted by anticancer therapy on several levels. First, the new selective pressures are expected to favor relatively treatment-resistant clonal subpopulations over sensitive ones, therefore limiting clonal diversity. Second, genotoxic treatments may elevate genomic instability, thereby potentially increasing cellular genetic diversity. Despite its clinical importance, the potential impact of cancer therapy on cellular genetic heterogeneity is largely unknown. Here, we report the effects of neoadjuvant chemotherapy on the extent of genetic and phenotypic cellular diversity within breast tumors and the associations between intratumor genetic heterogeneity and therapeutic outcomes.

RESULTS

Tumor-Subtype- and Cancer Cell-Type-Specific Differences in Genetic Diversity

To investigate relationships between intratumor heterogeneity and cancer therapy, we analyzed pre- and posttreatment tumor biopsies from 47 patients with breast cancer undergoing neoadjuvant chemotherapy (Table S1). These included 13 luminal A, 11 luminal B, 11 HER2+, and 12 TNBC (triple-negative breast cancer) tumors representing each of the major breast tumor subtypes (Perou et al., 2000). Four patients showed pathologic complete response (pCR) to treatment; thus, in these cases, posttreatment samples could not be analyzed.

Genetic heterogeneity was assessed based on immunofluorescence *in situ* hybridization (iIFISH) using BAC (bacterial artificial chromosome) probes for 8q24.3, 10p13, 16p13.3, and 20q13.31 and the corresponding centromeric probes (CEPs) to distinguish between gain of whole chromosomes versus specific chromosomal regions. These genomic loci were selected because they are the most commonly amplified chromosomal regions in breast cancer regardless of tumor subtype (e.g., 8q24) or within a specific tumor subtype (Nikolsky et al., 2008). Phenotypic heterogeneity was assessed by staining for CD44 and CD24 (Figure 1A) because prior studies from our and other laboratories demonstrated that these cell surface

Figure 1. Genetic Diversity in Breast Cancer According to Tumor Subtype and Treatment

- (A) Representative images of iIFISH in four tumors of the indicated subtypes before and after treatment.
- (B) Shannon index of diversity in each tumor subtype before and after treatment calculated based on unique BAC and CEP counts for each cell. Each dot represents an individual tumor, black line shows mean \pm SEM, and colors indicate luminal A (dark green), luminal B (light green), triple-negative (orange), and HER2+ (violet) tumor subtypes. Asterisks mark significant differences between subtypes: * $p \leq 0.05$ and ** $p \leq 0.01$, by Wilcoxon rank sum test.
- (C) Correlations between Shannon indices in each tumor before and after treatment and the relative change in diversity in each tumor. Black line shows mean \pm SEM.
- (D) Correlations between pre- and posttreatment Shannon indices in the indicated cell subpopulations and tumor subtypes. Not all cell subpopulations are present in all tumors.
- (E) Shannon index in phenotypically distinct subpopulations in individual tumors before and after treatment. Each vertical line separates individual cases. LumA, luminal A; LumB, luminal B; TN, triple negative.
- (F) Correlations between Shannon indices in each tumor before and after treatment for the indicated loci.

See also Figure S1 and Tables S1 and S2.

markers identify cancer cells with distinct molecular and biological properties (Al-Hajj et al., 2003; Bloushtain-Qimron et al., 2008; Li et al., 2008; Liu et al., 2007; Shipsitsin et al., 2007), including genetic heterogeneity both between and within CD44⁺ and CD24⁺ breast cancer cell populations (Park et al., 2010a; Shipsitsin et al., 2007). The neoplastic nature of the cells was confirmed by examining cellular and nuclear morphology using adjacent hematoxylin and eosin-stained slides and in the majority of cases by the presence of chromosomal copy number gain.

The 8q24 BAC and chromosome 8 (chr8) CEP signals were counted in about 100 individual cells for each of the four phenotypically distinct tumor cell populations (i.e., CD44⁺CD24⁻, CD44⁺CD24⁺, CD44⁻CD24⁺, and CD44⁻CD24⁻ cells). Diversity was evaluated based on Shannon and Simpson indices (Magurran, 2004) that were calculated in four different ways based on measures of (1) copy number of 8q24 (BAC probe), (2) copy number of chr8 centromeric region (CEP), (3) ratio of BAC/CEP counts, and (4) individual copy number of both BAC and CEP probes in each cell (unique counts). Overall, each of the four different calculations displayed similar relative differences among tumors and matched pre- and posttreatment samples, but diversity indices were the highest based on unique counts (Table S2). Thus, owing to its more accurate prediction of genetic diversity, we subsequently used unique counts for all analyses unless otherwise indicated.

First, we investigated whether pre- and posttreatment genetic diversity for 8q24 is different in distinct breast tumor subtypes. HER2+ tumors had significantly higher diversity after treatment compared to luminal B and TNBC tumors (Figure 1B; Table S2). However, there was no significant difference in overall genetic diversity in any of the tumors between pre- and posttreatment samples (Figure 1C). Next, we investigated potential changes in genetic diversity in phenotypically distinct tumor cell subpopulations. We required cell subpopulations for analysis to represent at least 5% of all cancer cells within a tumor in order to avoid a counting bias; thus, not all four phenotypic types were analyzed in all samples. In some tumors, we observed significant differences in the relative distribution of copy number for BAC or CEP probes or BAC/CEP ratios in specific cell subpopulations when comparing pre- and post-treatment data (Figure S1A). We also observed changes in cell populations and unique cancer cells based on kernel density estimates and Whittaker plots (Figures S1B and S1C). However, pairwise analysis of pre- and posttreatment differences in genetic diversity in each of the four phenotypic subpopulations across all tumors did not reveal significant changes (Figure 1D); cell-type-specific genetic diversity was significantly higher after treatment only in a few cases (Figure 1E; Table S2).

To ensure that our results were not due to the inaccurate reflection of overall genomic diversity based on 8q24 counts, we also analyzed three additional loci commonly amplified in luminal (16p13), TNBC (10p13), and HER2+ (20q13) tumors. Similar to 8q24, these additional loci also failed to demonstrate significant changes in genetic diversity (Figure 1F). Our data suggest that genetic diversity is an intrinsic tumor trait that remains relatively stable during treatment.

Changes in Phenotypic Heterogeneity Highlight Biologic Differences among Cell Types

To determine potential changes in cellular phenotypes due to treatment, we analyzed the relative frequency of the four distinct cell subpopulations within tumors. We observed a significant increase in the frequency of CD44⁻CD24⁺ cells in luminal A, luminal B, and TNBC tumors after treatment, and residual TNBC tumors were also enriched for CD44⁻CD24⁻ cells (Figures 2A and 2B). Concomitantly, there were fewer CD44⁺CD24⁻ cells in luminal A and triple-negative tumors after treatment, whereas HER2+ tumors displayed very few changes in the distribution of cell subpopulations. Next, we estimated the degree of phenotypic diversity based on the Shannon index and found that phenotypic diversity for CD44 and CD24 markers tends to decrease in luminal tumors, whereas it increases in TNBC tumors (Figure S2).

Because chemotherapy is thought to target proliferative cells (Collechi et al., 1998), the observed changes in the relative frequencies of the four cell subpopulations could be due to cell-type-specific differences in proliferation. Thus, we assessed the frequency of cells positive for the Ki67 proliferation marker within each of the four cell types before and after treatment. The fraction of Ki67⁺ cells was lower in all cell types in all tumors after treatment, with only a few exceptions (Figure S3A). We also observed significant differences in the proportion of Ki67⁺ cells before treatment between CD44⁺CD24⁻ and CD44⁻CD24⁺ cell populations, which were the most and least proliferative, respectively (Figures 2C and 2D). Spearman correlation analysis of associations between changes in the frequency of Ki67⁺ cells and cell subpopulations revealed a significant positive correlation in CD44⁺CD24⁻ cells ($p = 0.007$) and a significant negative correlation in CD44⁻CD24⁺ cells ($p < 0.001$) (Figure 2E). These results imply that the increase in the relative frequency of CD24⁺ compared to CD44⁺ cells after treatment might be due to the preferential elimination of the more proliferative CD44⁺ cells by chemotherapy. Thus, if a tumor remains highly proliferative after treatment, it has a higher CD44⁻CD24⁻-to-CD44⁺CD24⁺ cell ratio. However, the possibility of conversion from CD44⁺ to CD24⁺ cellular phenotypes or a change in the expression of these markers due to the cell-cycle phase or as a direct effect of treatment cannot be excluded. These results are in agreement with previous findings that treatment selects for slow-growing CD24⁺ cancer cells in lung cancer (Sharma et al., 2010) and in melanoma (Roesch et al., 2013).

Differences in cellular proliferation could also be related to differences in genetic diversity because faster-growing cells may have a larger population size and might therefore be more likely to accumulate genetic abnormalities. Thus, we also analyzed potential associations between the proliferation rate of each cell type and its genetic diversity index. Spearman correlation analysis demonstrated significant associations between Ki67 levels and the Shannon index of genetic diversity in CD44⁻CD24⁺ ($p = 0.007$) and CD44⁺CD24⁺ ($p = 0.027$) cells before treatment, suggesting that the observed genetic diversity in these cell subpopulations could be influenced by their lower proliferation rates (Figure S3B). In contrast, after treatment, Ki67 levels and Shannon indices showed a significant ($p = 0.04$) correlation only in CD44⁺CD24⁻ cells. We failed to observe

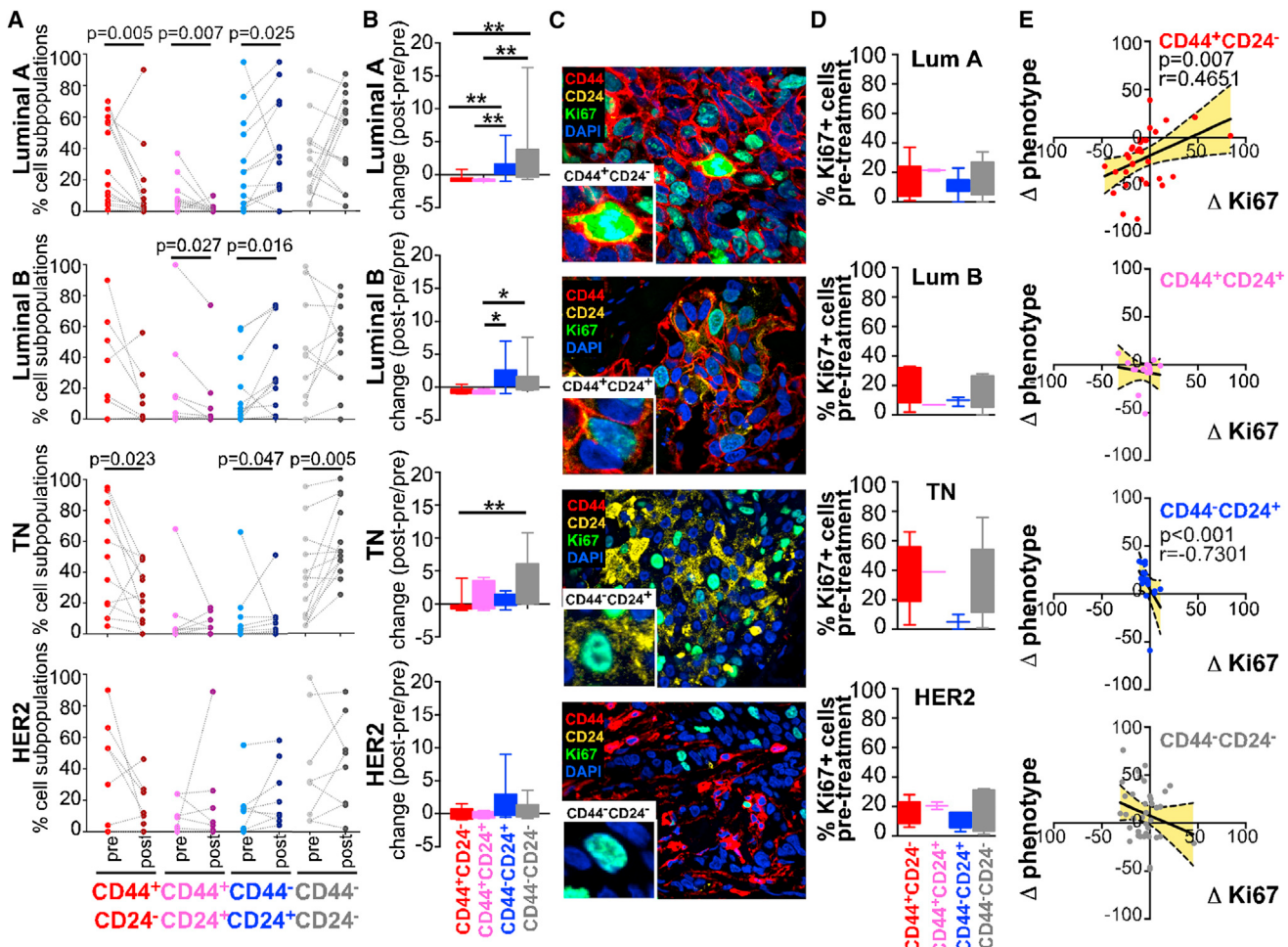


Figure 2. Changes in Phenotypic Heterogeneity and Cell-Type-Specific Variations in Proliferation Rates

(A) Changes in the frequency of the indicated cell subpopulations in the different tumor subtypes. Dotted line connects values for each cell subpopulation before and after treatment. Significant p values by two-sided Wilcoxon matched-pairs signed rank test are shown.

(B) Box plot depicts relative changes in the frequency of each of the four cell subpopulations. Boxes correspond to 25th–75th percentile, whereas whiskers mark maximum and minimum values. Asterisks indicate statistically significant differences by two-sided Wilcoxon matched-pairs signed rank test: *p < 0.05 and **p < 0.01.

(C) Representative immunofluorescence images of Ki67 staining in specific cell subpopulations.

(D) Frequency of Ki67⁺ cells before treatment. Boxes correspond to 25th–75th percentile, whereas whiskers mark maximum and minimum values.

(E) Correlation between differences (Δ denotes posttreatment minus pretreatment values) in the frequency of cell subpopulations and percentage (%) of Ki67⁺ cells after treatment. Negative values indicate a decrease of each variable after treatment. A 95% confidence interval is indicated in yellow.

See also Figures S2 and S3.

any associations between changes in diversity and changes in the fraction of Ki67⁺ cells during treatment (Figure S3C), suggesting that although differences in proliferation could be associated with differences in diversity in some cell subpopulations before treatment, changes in proliferation were not generally associated with differences in diversity after treatment.

Topology Maps to Explore Changes of Cellular Heterogeneity in Spatially Explicit Context

The previous analyses focused on population-level genotypic and phenotypic diversity. However, intermixing of tumor cells is substantially restricted in solid tumors by tissue architecture. Furthermore, heterogeneity of intratumor microenvironments, including differences in extracellular matrix and vascularization,

is expected to impact selective pressures and differentiation cues, thereby translating into differences in genotypes and phenotypes. Therefore, we decided to address whether accounting for spatially explicit tissue organization can reveal therapy-induced changes in cellular heterogeneity missed by population-based analyses. To investigate this issue, we created tumor topology maps by analyzing the distribution of cancer cells with distinct genotypes and phenotypes in three physically distinct regions in 15 tumors (5 of each of the 3 major subtypes) before and after treatment. These cases were selected based on the presence of sufficiently large cell numbers after treatment to allow cell-to-cell interaction analyses. For each cell, we recorded copy numbers of 8q24 BAC and chr8 CEP probes and cellular phenotype. Representative examples of such topology maps

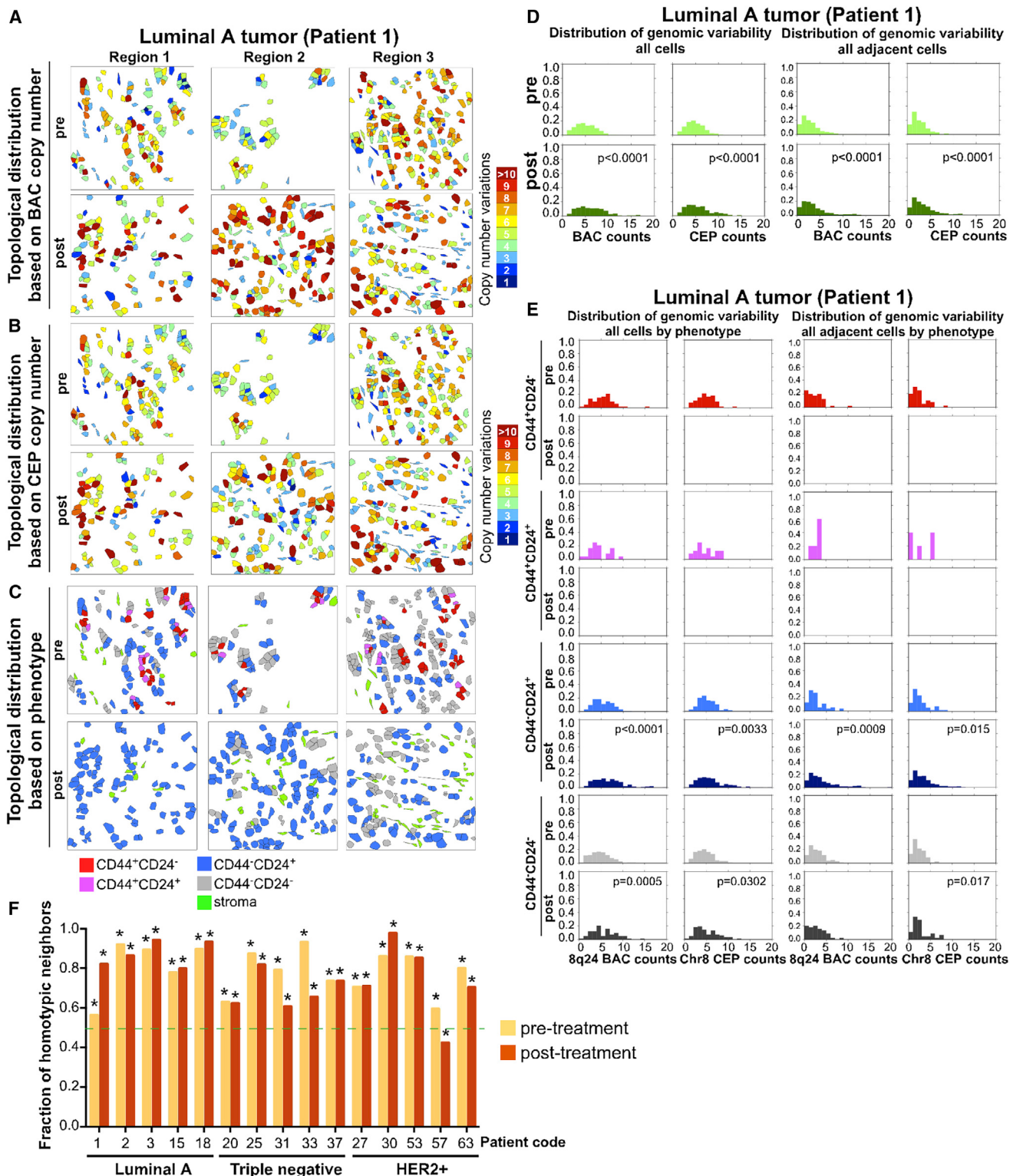


Figure 3. Analysis of Tumor Topology

(A–C) Maps showing topologic differences in the distribution of genetically distinct tumor cells based on copy number for 8q24 BAC (A), chr8 CEP (B), and cellular phenotype (C) in three different regions of a luminal A tumor (Patient 1).

(D) Histograms depicting absolute differences in copy numbers for BAC and CEP probe counts regardless of phenotype in all cells or in adjacent cells before and after treatment.

(legend continued on next page)

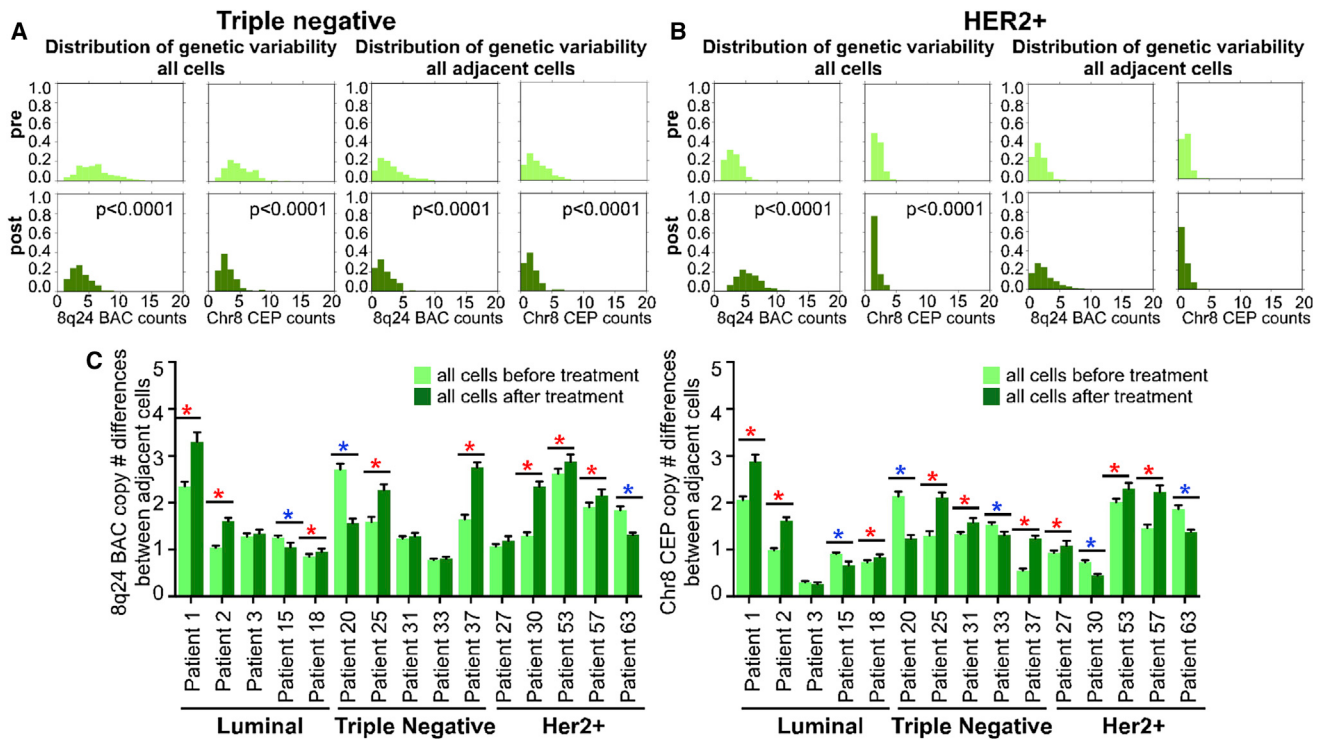


Figure 4. Genotype of All Cells and Adjacent Cells within Tumors

(A and B) Histograms depicting variability for 8q24 BAC and chr8 CEP probe counts regardless of phenotype in all cells (left panel) or in adjacent cells (right panel) before and after treatment in a triple-negative tumor (patient 20) (A) and in a HER2+ tumor (patient 30) (B).

(C) Summary of differences for 8q24 BAC or chr8 CEP probe counts in all cells before and after treatment in the 15 tumors analyzed. Asterisks mark significant differences, and red and blue color indicates increase and decrease in differences, respectively. Data are presented as mean \pm SEM.

are depicted in Figures 3A–3C (Patient 1, Luminal A tumor) and S4 (patient 20, TNBC, and patient 30, HER2+ tumor). The tumor of patient 1 showed a marked increase in both 8q24 BAC and chr8 CEP copy numbers and in the frequency of CD44⁺CD24[−] cells after treatment (Figures 3A–3C). In patient 20, there was a clear decrease in both 8q24 BAC and chr8 CEP copy numbers, but no substantial changes in the frequencies of cellular phenotypes (Figures S4A–S4C). In contrast, in patient 30, there was a dramatic increase in 8q24 BAC copy numbers with a concomitant decrease in chr8 CEP counts but essentially no changes in cellular phenotypes (Figures S4D–S4F). Therefore, at least some tumors display substantial phenotypic and genotypic differences pre- and posttreatment. Despite these changes, pre- and posttreatment genetic diversity indices in the three topologically distinct areas of each tumor were not significantly different (Table S3; Figure S5), with the exception of two cases (patients 1 and 3, both with partial response to treatment). These results imply that the analysis of even one region might be sufficient to assess overall genetic diversity of a tumor. However, because the distant regions we compared were still within one section and one biopsy, the possibility cannot be excluded

that biopsies taken from distant parts of the tumor may show more pronounced differences. Furthermore, the lack of significant differences in genetic diversity in different regions of the same tumor does not mean that tumor cells located in distinct areas are genetically identical. It rather implies that diversity is an inherent feature of the tumors that is less subjective to sampling bias than the measurement of a specific trait.

Effect of Treatment on the Distribution of Genetic Heterogeneity within Topology Maps

We then employed the topology maps to assess the effects of treatment on spatial distribution of genetic heterogeneity by measuring genetic distances between the adjacent and all cancer cells within tumors using the copy number differences for both 8q24 BAC and chr8 CEP. We observed that in most cases, the distribution of the differences in copy number was significantly different after treatment compared to before treatment, both when considering the differences only in adjacent cells or in all cells (Figures 3D and 4A). However, in some cases, the distribution of the differences in adjacent cells was not significantly different (Figure 4B), indicating the differential topologic

(E) Histograms depicting absolute differences in copy numbers for BAC and CEP probe counts in all cells of the same phenotype or in adjacent cells of the same phenotype before and after treatment. CD44⁺CD24[−] and CD44⁺CD24⁺ cell subpopulations are not present after treatment.

(F) Fraction of adjacent cells with the same phenotype before and after treatment. Asterisks indicate significant changes. Significance of differences was determined by calculating the homotypic fraction for 100,000 iterations of permutation testing over randomized cellular phenotypes. See also Figures S4 and S5 and Table S3.

distribution of cells with similar copy number. We observed that in several tumors, the genetic distance for both 8q24 BAC and chr8 CEP probes changed in the same direction after treatment, whereas in a few cases, the divergence for the 8q24 BAC probe decreased with a concomitant increase in variability for chr8 CEP (Figures 3D and 4A–4C). Overall, in the 15 tumors analyzed, the cell-to-cell variability for 8q24 BAC and chr8 CEP counts was significantly higher after treatment in eight cases, lower for chr8 CEP copy number in five patients, and decreased for 8q24 in three cases (Figure 4C). Therefore, incorporation of spatially explicit context into analysis of genetic diversity has revealed differences missed by population-wide analysis. However, the causes of the observed differences are difficult to interpret because increase in copy number differences between adjacent cells after chemotherapy could be due to an increase in genetic instability, the selection for slowly proliferating cells that are more likely to be phylogenetically distinct, or increased cell migration.

We then sought to obtain further insight by analyzing changes in genetic divergence within cells with similar phenotype focusing on the four phenotypically distinct cellular subpopulations defined by expression of CD24 and CD44. We found significant cell-type-specific differences in the degree of genetic variability between all cells and all adjacent cells of the same phenotype within individual tumors. For example, in a luminal tumor (patient 1), the increase in cell-to-cell variability for 8q24 and chr8 CEP copy numbers was significant in CD44[−]CD24⁺ and CD44[−]CD24[−] cells when considering all cells, whereas in adjacent cells, only the CD44[−]CD24⁺ fraction showed a significant increase for both BAC and CEP probes (Figure 3E). In this tumor, we could not detect any CD44⁺CD24[−] and CD44⁺CD24⁺ cells after treatment. Thus, it is possible that the increased genetic heterogeneity of the CD44[−]CD24⁺ and CD44[−]CD24[−] fractions was due to phenotypic switch of the CD44⁺ cell populations due to treatment.

Similarly, in a TNBC (patient 20), variability for 8q24 and chr8 CEP counts decreased in all CD44⁺CD24[−] and CD44[−]CD24[−] cells (adjacent or not), but in CD44⁺CD24⁺ cells, the variability for 8q24 only decreased in adjacent cells (Figures 5A and 5B). Similar differences were observed in other cases for changes in genetic variability between adjacent cells compared to all cells within the tumor, like in a HER2+ tumor (patient 30) (Figures 5B and 5C).

The increased genetic variability in adjacent cells of the same phenotype together with the significant changes in the relative frequency of distinct cell subpopulations due to treatment suggests either selection for distinct phenotypes based on their differential sensitivity to the treatment or increased rates of genomic instability resulting from the treatment. Interestingly, in all 15 tumors analyzed, the frequency of homotypic-phenotypic clustering was significantly higher compared to the heterotypic one both before and after treatment (Figure 3F). Thus, tumor cells tend to cluster more based on their phenotype than on their genotype. The results of these topology analyses highlight the insights afforded by analyzing tumors at the single-cell level and *in situ* because the spatial organization of the cells with distinct genotypes and phenotypes is lost when analyzing bulk tissues or dissociated cells.

Computational Modeling Allows an Investigation of Tumor Growth Patterns and Evolution during Treatment

To better understand the forces that could give rise to the observed patterns of spatial clustering of cells with the same phenotype, we next developed a stochastic computational model of cellular proliferation and death utilizing our tumor topology and Ki67 data (see *Supplemental Experimental Procedures* for details). This model is based on a stochastic process of cell growth and death in a 2D cross-section of a tumor, implemented as a patient-specific computer simulation informed by parameters measured in a patient-specific manner. This model was used to investigate the growth patterns and evolutionary dynamics of tumor cells during chemotherapy and also enabled us to determine the extent to which proliferation alone could explain the detected clustering of phenotypes.

The initialization state for the simulation for each patient consisted of the cell coordinates for each cell in the pretreatment samples, an estimation of the age of each cell based on its size, and the cellular phenotypes. We considered the average length of the cell cycle across all cellular phenotypes and all patients to be comparable to the average cell-cycle time determined by cell line experiments (Schiffer et al., 1979), and then varied individual cell-cycle times based on the corresponding Ki67 values. Initially, we assumed that daughter cells maintained the same phenotype as the mother cell, thus neglecting the possibility of phenotypic switching or migration; this assumption was later relaxed.

Each patient-specific simulation was performed for three phases of proliferation. The first phase consisted of the period of time between biopsy and start of chemotherapy. Cell proliferation occurred at the rates determined by the pretreatment Ki67 data. The probability of cell death per unit time for each phenotype was selected to maintain a roughly constant population size. We chose these values for cell death because rates of apoptosis correlate well with proliferation, and the montage of visualized cells did not consist of cells crowded together as would be consistent with high growth rates. During treatment, we lowered proliferation by 5% and adjusted the rate of cell death accordingly. This choice of treatment effect was selected by fitting the number of cells at the end of the simulation to the number of cells observed in the posttreatment samples, and due to evidence of a decrease in proliferation with anthracyclines with a corresponding decrease in apoptotic index (Burcombe et al., 2006). The last phase consisted of the period of time between the end of chemotherapy and surgery. Cell proliferation in this phase occurred at the rates determined by the post-treatment Ki67 data (Figure 6). These three time periods were obtained individually for each patient and implemented in the patient-specific simulations.

Using this model, we found that the level of clustering detected in our posttreatment samples was less than what would be expected in a model without cellular motility or phenotypic switching (Figure 6; Table S4; Movie S1). Therefore, we sought to determine rates of phenotypic switching that would fit the distribution of cell types found in our post-treatment samples. We identified a lower requirement for phenotypic switching or motility among the luminal tumors, whereas we observed both low and high rates for patients

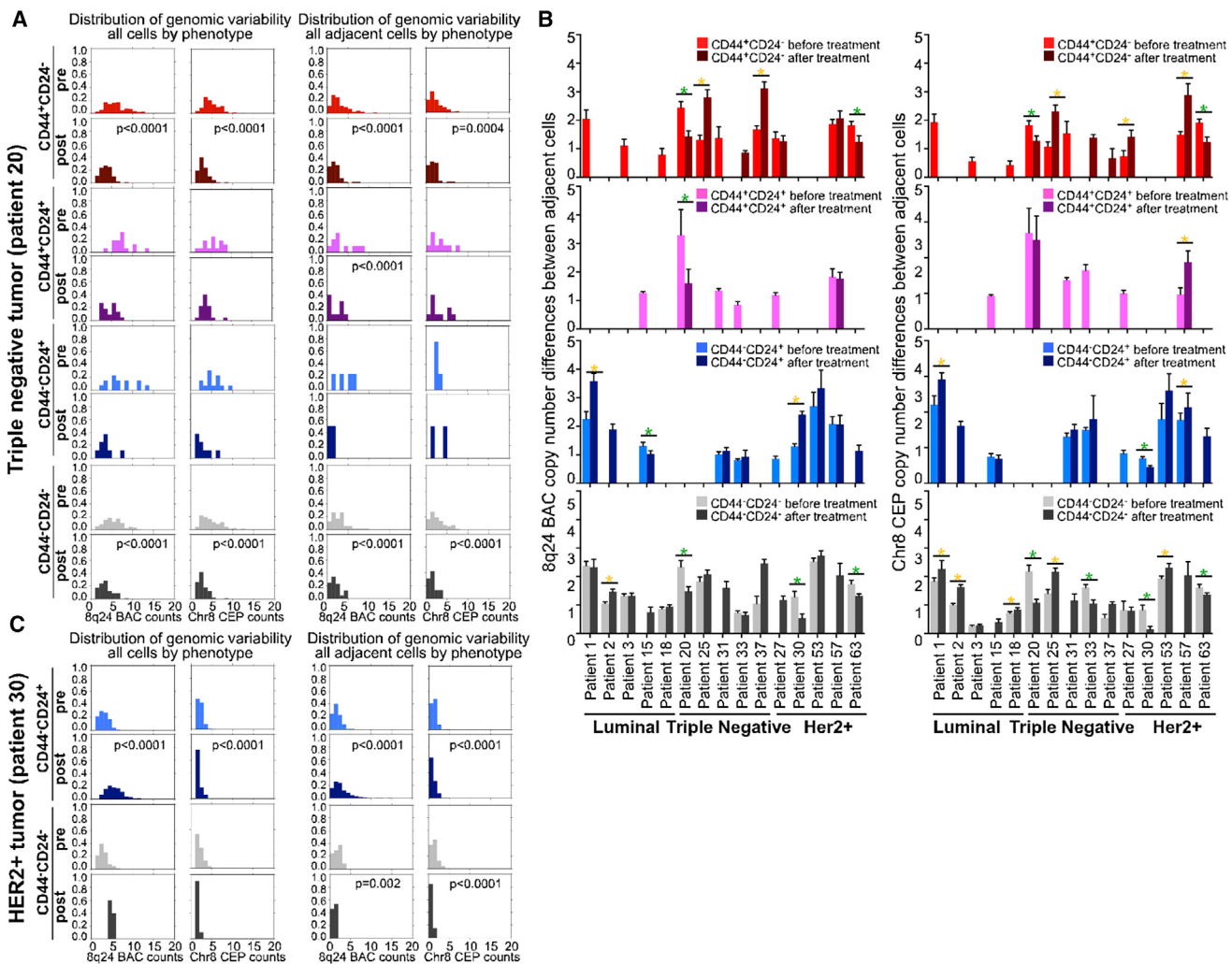


Figure 5. Genetic and Phenotypic Differences between All Cells and Adjacent Cells

(A) Histograms depicting variability for 8q24 BAC and chr8 probe counts in all cells of the same phenotype (left panel) or in adjacent cells of the same phenotype (right panel) before and after treatment in a triple-negative tumor (patient 20).

(B) Plots depicting differences in 8q24 BAC and chr8 CEP copy number in all adjacent cells and in adjacent cells of the same phenotype. Asterisks indicate significant differences, and yellow and green color indicates increase and decrease in differences, respectively. Data are presented as mean \pm SEM.

(C) Similar as (A), histograms for a HER2+ tumor (patient 30).

with HER2+ and triple-negative tumors (see [Supplemental Experimental Procedures](#) for more details). The inclusion of migration in this model, based on intravital imaging of metastatic breast cancer cells ([Kedrin et al., 2008](#)), led to increases in the rates of phenotypic switching necessary to recapitulate the posttreatment data but did not change the relative ordering of the breast tumor subtypes with regard to this rate. Migration was assumed to occur in a nondirected manner (i.e., in random directions) and was considered to be higher for CD44⁺ CD24⁻ and CD44⁺ CD24⁺ cells as compared to CD44⁻ CD24⁺ and CD44⁻ CD24⁻ cells. This model provides a proof of principle of feasibility of the prediction of therapy-induced phenotypic changes in tumor based on the detailed characterization of tissue samples at the single-cell level before and after treatment.

The Impact of Intratumor Diversity on Therapeutic Responses

To explore the potential impact of intratumor diversity on therapeutic resistance, we compared genetic and phenotypic diversity among tumors classified as pCR and pathological partial response (pPR) or stable disease. Interestingly, tumors with pCR had the lowest pretreatment genetic diversity using measures that incorporated 8q24 copy number, whereas tumors with partial response or stable disease were not significantly different from each other, neither before nor after treatment ([Figures 7 and S6A; Table S5](#)).

Age at diagnosis affects both breast tumor subtype and the success of chemotherapy within a subtype ([Hess et al., 2006](#)). TNBC is more common in younger women, and chemotherapy also tends to be more effective in younger patients ([Silver](#)

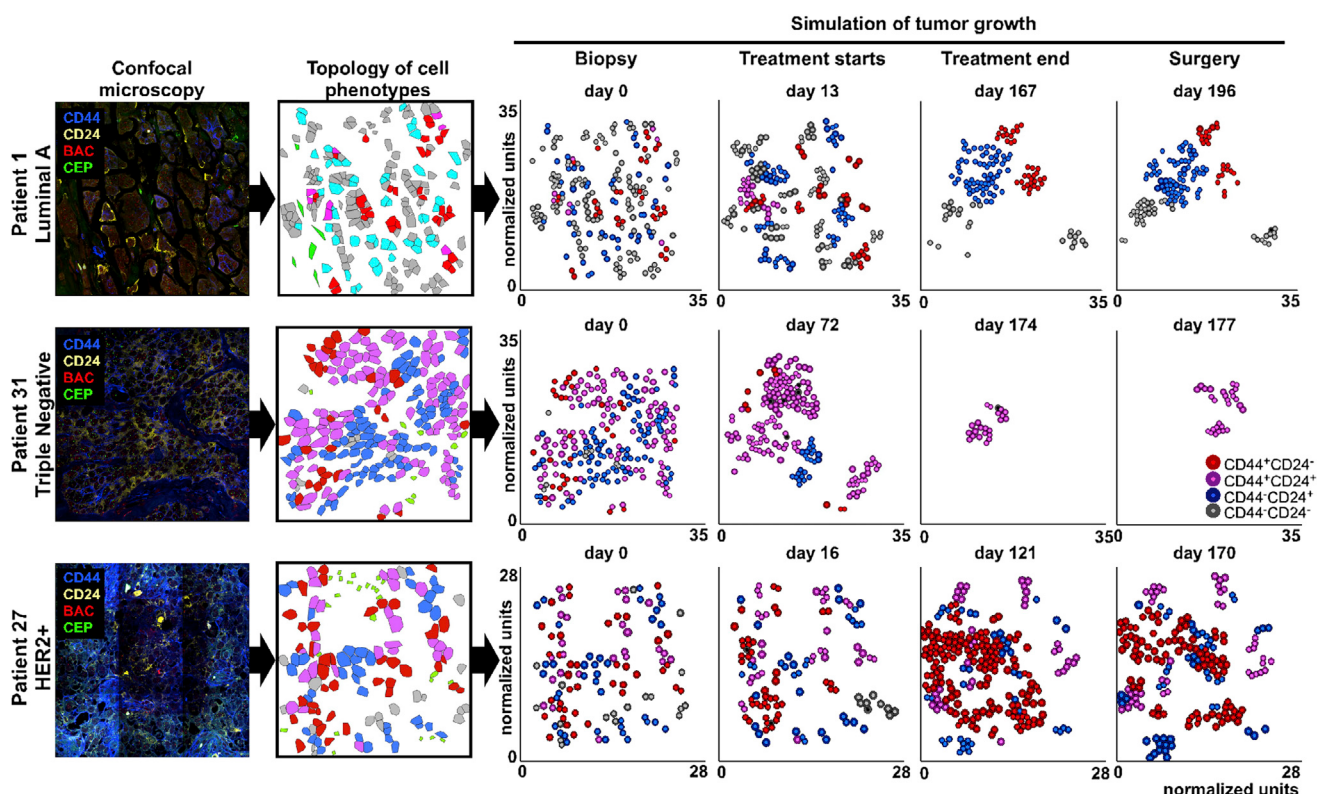


Figure 6. Examples of Snapshots of Computer-Simulated Tumor Growth during Treatment

Representative images depicting changes in tumor topology and cellular composition during treatment based on simulations. Modeling was built based on actual data obtained from cases analyzed for topology. Confocal images were converted into topology maps for the distribution of cell phenotypes that served as time zero for the mathematical simulations of tumor growth. See also Table S4 and Movie S1.

et al., 2010). These epidemiological data suggest that tumors of different subtypes may have different evolutionary paths and growth kinetics such as the length of time from tumor initiation to diagnosis, which may influence both treatment responses and intratumor heterogeneity. Thus, we analyzed potential associations between the age at diagnosis and the Shannon diversity index of each tumor. We found that the extent of pre-treatment diversity did not display a significant correlation with patient age (Figure S6B). However, older age at diagnosis was significantly correlated with a decrease in genetic diversity during treatment in TNBC ($p = 0.025$) and an increase in genetic diversity in HER2+ tumors ($p = 0.038$; Figure S6C). These results suggest that TNBC in older women may have a dominant, slowly proliferating subpopulation that is resistant to treatment, whereas HER2+ tumors in older women might be more genetically unstable.

It is possible that treatment-induced changes in genetic diversity might be masked by rediversification during the time interval between the end of treatment and posttreatment sample collection (i.e., surgery). Similarly, the duration of the treatment (i.e., length of selective pressure) might affect intratumor genetic diversity. Thus, we analyzed potential associations between these clinical variables and changes in genetic diversity but did not detect any significant associations (Figures S6D and S6E). These results suggest that the observed lack of changes in ge-

netic diversity during neoadjuvant chemotherapy is not likely to be affected by the lengths of treatment and time between the last dose of chemotherapy and the surgical removal of residual tumors.

DISCUSSION

Here, we describe a single-cell-based analysis of intratumor genetic and phenotypic diversity and topology in a cohort of breast tumors prior to and after neoadjuvant chemotherapy. Although inter- and intratumor heterogeneity has been described and well characterized in breast cancer (Cancer Genome Atlas Network, 2012; Geyer et al., 2010; Hernandez et al., 2012; Polyak, 2011; Stephens et al., 2012; Yap et al., 2012), our knowledge of how intratumor heterogeneity may change during therapeutic interventions in distinct subtypes of breast cancers is very limited.

Neoadjuvant (i.e., preoperative) chemotherapy is a well-established standard treatment option for patients diagnosed with locally advanced disease or patients with large potentially operable tumors (Kaufmann et al., 2006). In addition to its effectiveness in reducing the size of the primary tumor, allowing for less-extensive surgery, neoadjuvant chemotherapy also improves long-term clinical outcome, presumably by eliminating micrometastatic disease (Fisher et al., 1998). Moreover,

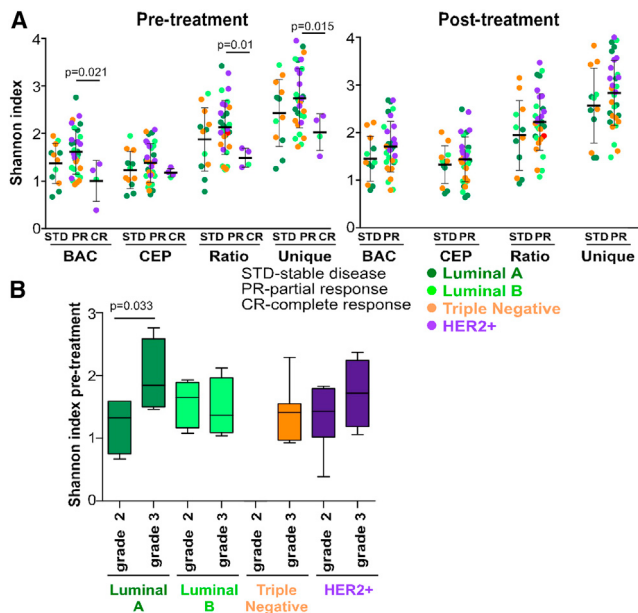


Figure 7. Associations between Intratumor Diversity and Pathologic Response to Treatment

(A) Shannon index of diversity before and after treatment in tumors with different response to treatment. Significant p values between groups by the Wilcoxon rank sum test are indicated. Black lines show the mean \pm SEM. Tumors with lower pretreatment diversity are more likely to have pCR regardless of tumor subtype. Tumors with pCR were only analyzed prior to treatment because there was no tumor tissue left at the time of surgery.

(B) Shannon index of diversity before and after treatment in tumors with different grade. Boxes correspond to 25th-75th percentile, whereas whiskers mark maximum and minimum values. Significant p values by two-sided Wilcoxon matched-pairs signed rank test are shown.

See also Figure S6 and Table S5.

a pCR to neoadjuvant treatment is a strong predictor of long-term disease-free survival (Esserman et al., 2012), particularly in estrogen receptor (ER)-negative cancers. Despite widespread use of neoadjuvant therapies, our knowledge of their influence on the subsequent evolution of the tumors is very limited.

The success of chemotherapy is influenced by breast tumor subtype, with luminal tumors in general being less responsive than HER2+ and TNBC (Houssami et al., 2012). Because chemotherapy is thought to target proliferating cells, associations between tumor proliferation (measured by the Ki67 index) and treatment response have been extensively characterized, with conflicting results. A recent study found that the relative change in the fraction of Ki67⁺ cells, but not the absolute pre- and post-treatment levels of Ki67⁺ cells, is an independent predictor of treatment outcomes after neoadjuvant chemotherapy in luminal B, HER2+, and TBNC subtypes (Matsubara et al., 2013). Changes in hormone receptors and HER2 due to neoadjuvant therapy have also been analyzed with inconclusive results (van de Ven et al., 2011).

More recently, intratumor heterogeneity for cellular phenotypes, mainly focusing on stem cell-like and more differentiated cell features, has been explored as a potential predictor of the

success of neoadjuvant chemotherapy. The frequency of CD44⁺ stem cell-like and CD24⁺ more-differentiated breast cancer cells varies within tumors according to subtype, with CD44⁺ cells being more common in TNBCs than in luminal cancers (Honeth et al., 2008; Park et al., 2010b). The relative frequency of these cells within tumors also changes during neoadjuvant chemotherapy. A study analyzing pre- and posttreatment samples by fluorescence-activated cell sorting (FACS) found an increase in CD44⁺CD24⁻ cells; however, the neoplastic nature of these cells was not confirmed (Li et al., 2008). Another report found that whereas an increased frequency of CD44⁺CD24⁻ cells after neoadjuvant chemotherapy was a poor prognostic factor, tumors that had a high fraction of these cells were more likely to have a pCR (Lee et al., 2011).

Here, we showed that whereas overall intratumor cellular genetic diversity for 8q24, 16p13, 10p13, and 20q does not change during treatment in tumors with a partial or no response, there are significant changes in phenotypically distinct tumor cell subpopulations within tumors and in the relative localization of these populations of cells. Some of these changes might be explained by the observed differences in the proliferation rates among cell types, with CD44⁺CD24⁻ cells being more proliferative and thus more likely to be eliminated. Our data, however, also imply potential changes in cellular phenotypes and selection for cells with more differentiated luminal features due to lower sensitivity to the therapy stemming from lower proliferation capacity. Moreover, our findings provide a potential explanation for the apparent paradox between the presumed resistance of CD44⁺ stem cell-like breast cancer cells (i.e., cancer stem cells) (Dave et al., 2012) and our data demonstrating a relative decrease in this cell population due to treatment. Based on our data, CD44⁺CD24⁻ cells are more proliferative than CD44⁻CD24⁺ cells, and thus, they might be preferentially eliminated by chemotherapy. If a tumor does not respond to treatment due to inherent resistance, which is independent of stem cell-like or epithelial phenotype, then there is an apparent increase in the relative frequency of CD44⁺CD24⁻ cells due to their higher proliferation.

Our observation that in some cases adjacent cells within a tumor are more likely to be genetically divergent yet phenotypically similar implies that homotypic cell-cell interactions might favor treatment resistance and also that chemotherapy might increase genetic instability or select for cells with higher chromosomal instability.

Our computational model of tumor cell proliferation provides a tool with which we can predict changes in the distribution of cell phenotypes in a patient-specific fashion. These variations can manifest themselves in spatial coordinates and clustering of cells, or they can be the result of changing population dynamics over periods of time with and without therapy. Here, we found that the clustering of cellular phenotypes could not have occurred solely due to cell division placing daughter cells closer to the parent cell but must require some level of phenotypic plasticity. We tested varying levels of phenotypic switching and found that no single rate of switching could account for the divergence between simulation and biopsy samples: instead, rates of switch may vary at the subtype or individual patient level. We

also investigated the effects of migration on the predicted levels of phenotypic switching and found that migration increases the rate of phenotype switching necessary to explain the patient data. This effect might arise because migration scatters cells more widely throughout the tumor, and hence, phenotype switching is needed to return the patterns of cells to those observed in patient samples.

In summary, our data provide an integrated view of how the genotype (measured by 8q24 copy number), phenotype (CD24 and CD44 expression and proliferation state), and topology (distribution of cancer cells with defined genotype and phenotype within tumors) change in response to neoadjuvant chemotherapy in breast cancer. Because phenotypic diversity in combination with selection pressure by local microenvironmental signals is the driver of tumor evolution, our results highlight the importance of using an integrated approach. Finally, our *in silico* simulation of tumor growth using models built on the patient-specific characterization of tumors at the single-cell level *in situ* prior to and after chemotherapy illustrates the feasibility of predicting the evolution of tumors during treatment—knowledge that could be used for the design of more effective treatment strategies.

EXPERIMENTAL PROCEDURES

For further details, see the [Supplemental Experimental Procedures](#).

ImmunoFISH

The use and collection of the human tissue samples were performed following protocols approved by the institutional review boards of the hospitals participating in this study. Formalin-fixed paraffin-embedded breast tumor samples were dewaxed in xylene and hydrated in a series of ethanol. Heat-induced antigen retrieval was performed in citrate buffer (pH 6), followed by pepsin digestion. The immunostaining for CD44 and CD24 was performed at room temperature, followed by the hybridization with BAC and CEP probes and incubation for 20 hr at 37°C. After several washes with different stringent SCC buffers, the slides were air-dried and protected for long storage with ProLong Gold. Different immunofluorescence images from multiple areas of each sample were acquired with a Nikon Ti microscope attached to a Yokogawa spinning-disk confocal unit, 60× plan apo objective, and OrcaER camera controlled by Andor iQ software.

Immunofluorescence Analysis of Cellular Phenotypes and Proliferation

Multicolor immunofluorescence for CD44, CD24, and Ki67 was performed using whole sections of formalin-fixed paraffin-embedded breast tumor samples by sequential staining after antigen retrieval in citrate buffer (pH 6). Different immunofluorescence images were acquired as described before, and the frequency of each cell phenotype was calculated by counting an average of 300 cells in each sample.

Statistical Analyses

Genetic diversity was determined as described by [Park et al. \(2010a\)](#). Statistical differences in genetic diversity were analyzed by bootstrapping and comparing the mean count of each bootstrap repetition against the mean count of the smaller cell population. Correlations were assessed using Spearman's rank-based coefficient. The association between diversity indices and clinical variables was assessed using the Wilcoxon test for categorical clinical variables (such as response) and a permutation test based on Spearman's rank correlation for continuous clinical variables (such as size). Statistical differences in pre- and posttreatment BAC and CEP counts were evaluated using the achieved significance level (ASL) method of [Efron and Tibshirani \(1993\)](#).

SUPPLEMENTAL INFORMATION

Supplemental Information includes Supplemental Experimental Procedures, six figures, five tables, and one movie and can be found with this article online at <http://dx.doi.org/10.1016/j.celrep.2013.12.041>.

ACKNOWLEDGMENTS

We thank members of our laboratories for their critical reading of this manuscript and useful discussions. We thank Lisa Cameron in the DFCI Confocal Microscopy for her technical support. This work was supported by the National Cancer Institute Physical Sciences Oncology Center U54CA143874 (to A.v.O.) and U54CA143798 (to F.M.), the Susan G. Komen Foundation (to R.M.), Cellex Foundation (to V.A.), by Redes Temáticas de Investigación en Cáncer (RD12/0036/0055 to P.G. and E.A.), and the Breast Cancer Research Foundation (to K.P.). Part of this work was performed under the auspices of the U.S. Department of Energy by Lawrence Livermore National Laboratory under Contract DE-AC52-07NA27344.

Received: June 14, 2013

Revised: November 14, 2013

Accepted: December 30, 2013

Published: January 23, 2014

REFERENCES

- Al-Hajj, M., Wicha, M.S., Benito-Hernandez, A., Morrison, S.J., and Clarke, M.F. (2003). Prospective identification of tumorigenic breast cancer cells. *Proc. Natl. Acad. Sci. USA* **100**, 3983–3988.
- Almendro, V., Marusyk, A., and Polyak, K. (2013). Cellular heterogeneity and molecular evolution in cancer. *Annu. Rev. Pathol.* **8**, 277–302.
- Bloushtain-Qimron, N., Yao, J., Snyder, E.L., Shipitsin, M., Campbell, L.L., Mani, S.A., Hu, M., Chen, H., Ustyancky, V., Antosiewicz, J.E., et al. (2008). Cell type-specific DNA methylation patterns in the human breast. *Proc. Natl. Acad. Sci. USA* **105**, 14076–14081.
- Burcombe, R., Wilson, G.D., Dowsett, M., Khan, I., Richman, P.I., Daley, F., Detre, S., and Makris, A. (2006). Evaluation of Ki-67 proliferation and apoptotic index before, during and after neoadjuvant chemotherapy for primary breast cancer. *Breast Cancer Res.* **8**, R31.
- Cancer Genome Atlas Network (2012). Comprehensive molecular portraits of human breast tumours. *Nature* **490**, 61–70.
- Collecchi, P., Baldini, E., Giannessi, P., Naccarato, A.G., Passoni, A., Gardin, G., Roncella, M., Evangelista, G., Bevilacqua, G., and Conte, P.F. (1998). Primary chemotherapy in locally advanced breast cancer (LABC): effects on tumour proliferative activity, bcl-2 expression and the relationship between tumour regression and biological markers. *Eur. J. Cancer* **34**, 1701–1704.
- Dave, B., Mittal, V., Tan, N.M., and Chang, J.C. (2012). Epithelial-mesenchymal transition, cancer stem cells and treatment resistance. *Breast Cancer Res.* **14**, 202.
- Ding, L., Ley, T.J., Larson, D.E., Miller, C.A., Koboldt, D.C., Welch, J.S., Ritchev, J.K., Young, M.A., Lamprecht, T., McLellan, M.D., et al. (2012). Clonal evolution in relapsed acute myeloid leukaemia revealed by whole-genome sequencing. *Nature* **481**, 506–510.
- Efron, B., and Tibshirani, R.J. (1993). *An Introduction to the Bootstrap* (London: Chapman & Hall).
- Engelman, J.A., Zejnullah, K., Mitsudomi, T., Song, Y., Hyland, C., Park, J.O., Lindeman, N., Gale, C.M., Zhao, X., Christensen, J., et al. (2007). MET amplification leads to gefitinib resistance in lung cancer by activating ERBB3 signaling. *Science* **316**, 1039–1043.
- Esserman, L.J., Berry, D.A., DeMichele, A., Carey, L., Davis, S.E., Buxton, M., Hudis, C., Gray, J.W., Perou, C., Yau, C., et al. (2012). Pathologic complete response predicts recurrence-free survival more effectively by cancer subset: results from the I-SPY 1 TRIAL—CALGB 150007/150012, ACRIN 6657. *J. Clin. Oncol.* **30**, 3242–3249.

- Fidler, I.J. (1978). Tumor heterogeneity and the biology of cancer invasion and metastasis. *Cancer Res.* 38, 2651–2660.
- Fisher, B., Bryant, J., Wolmark, N., Mamounas, E., Brown, A., Fisher, E.R., Wickerham, D.L., Begovic, M., DeCillis, A., Robidoux, A., et al. (1998). Effect of preoperative chemotherapy on the outcome of women with operable breast cancer. *J. Clin. Oncol.* 16, 2672–2685.
- Gerlinger, M., Rowan, A.J., Horswell, S., Larkin, J., Endesfelder, D., Gronroos, E., Martinez, P., Matthews, N., Stewart, A., Tarpey, P., et al. (2012). Intratumor heterogeneity and branched evolution revealed by multiregion sequencing. *N. Engl. J. Med.* 366, 883–892.
- Geyer, F.C., Weigelt, B., Natrajan, R., Lambros, M.B., de Biase, D., Vatcheva, R., Savage, K., Mackay, A., Ashworth, A., and Reis-Filho, J.S. (2010). Molecular analysis reveals a genetic basis for the phenotypic diversity of metaplastic breast carcinomas. *J. Pathol.* 220, 562–573.
- Heppner, G.H., and Miller, B.E. (1983). Tumor heterogeneity: biological implications and therapeutic consequences. *Cancer Metastasis Rev.* 2, 5–23.
- Hernandez, L., Wilkerson, P.M., Lambros, M.B., Campion-Flora, A., Rodrigues, D.N., Gauthier, A., Cabral, C., Pawar, V., Mackay, A., A'hern, R., et al. (2012). Genomic and mutational profiling of ductal carcinomas *in situ* and matched adjacent invasive breast cancers reveals intra-tumour genetic heterogeneity and clonal selection. *J. Pathol.* 227, 42–52.
- Hess, K.R., Anderson, K., Symmans, W.F., Valero, V., Ibrahim, N., Mejia, J.A., Booser, D., Theriault, R.L., Buzdar, A.U., Dempsey, P.J., et al. (2006). Pharmacogenomic predictor of sensitivity to preoperative chemotherapy with paclitaxel and fluorouracil, doxorubicin, and cyclophosphamide in breast cancer. *J. Clin. Oncol.* 24, 4236–4244.
- Honeth, G., Bendahl, P.O., Ringnér, M., Saal, L.H., Gruvberger-Saal, S.K., Lövgren, K., Grabau, D., Fernö, M., Borg, A., and Hegardt, C. (2008). The CD44+/CD24- phenotype is enriched in basal-like breast tumors. *Breast Cancer Res.* 10, R53.
- Houssami, N., Macaskill, P., von Minckwitz, G., Marinovich, M.L., and Mamounas, E. (2012). Meta-analysis of the association of breast cancer subtype and pathologic complete response to neoadjuvant chemotherapy. *Eur. J. Cancer* 48, 3342–3354.
- Kaufmann, M., Hortobagyi, G.N., Goldhirsch, A., Scholl, S., Makris, A., Valagussa, P., Blohmer, J.U., Eiermann, W., Jackes, R., Jonat, W., et al. (2006). Recommendations from an international expert panel on the use of neoadjuvant (primary) systemic treatment of operable breast cancer: an update. *J. Clin. Oncol.* 24, 1940–1949.
- Kedrin, D., Gligorijevic, B., Wyckoff, J., Verkhusha, V.V., Condeelis, J., Segall, J.E., and van Rheenen, J. (2008). Intravital imaging of metastatic behavior through a mammary imaging window. *Nat. Methods* 5, 1019–1021.
- Landau, D.A., Carter, S.L., Getz, G., and Wu, C.J. (2013). Clonal evolution in hematological malignancies and therapeutic implications. *Leukemia*. Published online August 27, 2013. <http://dx.doi.org/10.1038/leu.2013.248>.
- Lee, H.E., Kim, J.H., Kim, Y.J., Choi, S.Y., Kim, S.W., Kang, E., Chung, I.Y., Kim, I.A., Kim, E.J., Choi, Y., et al. (2011). An increase in cancer stem cell population after primary systemic therapy is a poor prognostic factor in breast cancer. *Br. J. Cancer* 104, 1730–1738.
- Li, X., Lewis, M.T., Huang, J., Gutierrez, C., Osborne, C.K., Wu, M.F., Hilsenbeck, S.G., Pavlick, A., Zhang, X., Chamness, G.C., et al. (2008). Intrinsic resistance of tumorigenic breast cancer cells to chemotherapy. *J. Natl. Cancer Inst.* 100, 672–679.
- Liu, R., Wang, X., Chen, G.Y., Dalerba, P., Gurney, A., Hoey, T., Sherlock, G., Lewicki, J., Shedd, K., and Clarke, M.F. (2007). The prognostic role of a gene signature from tumorigenic breast cancer cells. *N. Engl. J. Med.* 356, 217–226.
- Magurran, A.E. (2004). *Measuring Biological Diversity* (Malden: Blackwell).
- Maley, C.C., Galipeau, P.C., Finley, J.C., Wongsurawat, V.J., Li, X., Sanchez, C.A., Paulson, T.G., Blount, P.L., Risques, R.A., Rabinovitch, P.S., and Reid, B.J. (2006). Genetic clonal diversity predicts progression to esophageal adenocarcinoma. *Nat. Genet.* 38, 468–473.
- Marusyk, A., and Polyak, K. (2010). Tumor heterogeneity: causes and consequences. *Biochim. Biophys. Acta* 1805, 105–117.
- Marusyk, A., Almendro, V., and Polyak, K. (2012). Intra-tumour heterogeneity: a looking glass for cancer? *Nat. Rev. Cancer* 12, 323–334.
- Matsubara, N., Mukai, H., Fujii, S., and Wada, N. (2013). Different prognostic significance of Ki-67 change between pre- and post-neoadjuvant chemotherapy in various subtypes of breast cancer. *Breast Cancer Res. Treat.* 137, 203–212.
- Merlo, L.M., Pepper, J.W., Reid, B.J., and Maley, C.C. (2006). Cancer as an evolutionary and ecological process. *Nat. Rev. Cancer* 6, 924–935.
- Merlo, L.M., Shah, N.A., Li, X., Blount, P.L., Vaughan, T.L., Reid, B.J., and Maley, C.C. (2010). A comprehensive survey of clonal diversity measures in Barrett's esophagus as biomarkers of progression to esophageal adenocarcinoma. *Cancer Prev. Res. (Phila.)* 3, 1388–1397.
- Mroz, E.A., Tward, A.D., Pickering, C.R., Myers, J.N., Ferris, R.L., and Rocco, J.W. (2013). High intratumor genetic heterogeneity is related to worse outcome in patients with head and neck squamous cell carcinoma. *Cancer* 119, 3034–3042.
- Navin, N., Kendall, J., Troge, J., Andrews, P., Rodgers, L., McIndoo, J., Cook, K., Stepansky, A., Levy, D., Esposito, D., et al. (2011). Tumour evolution inferred by single-cell sequencing. *Nature* 472, 90–94.
- Nazarian, R., Shi, H., Wang, Q., Kong, X., Koya, R.C., Lee, H., Chen, Z., Lee, M.K., Attar, N., Sazegar, H., et al. (2010). Melanomas acquire resistance to B-Raf(V600E) inhibition by RTK or N-RAS upregulation. *Nature* 468, 973–977.
- Nikolsky, Y., Sviridov, E., Yao, J., Dosymbekov, D., Ustyansky, V., Kaznacheev, V., Dezso, Z., Mulvey, L., Macconail, L.E., Winckler, W., et al. (2008). Genome-wide functional synergy between amplified and mutated genes in human breast cancer. *Cancer Res.* 68, 9532–9540.
- Park, S.Y., Gönen, M., Kim, H.J., Michor, F., and Polyak, K. (2010a). Cellular and genetic diversity in the progression of *in situ* human breast carcinomas to an invasive phenotype. *J. Clin. Invest.* 120, 636–644.
- Park, S.Y., Lee, H.E., Li, H., Shipsits, M., Gelman, R., and Polyak, K. (2010b). Heterogeneity for stem cell-related markers according to tumor subtype and histologic stage in breast cancer. *Clin. Cancer Res.* 16, 876–887.
- Perou, C.M., Sørlie, T., Eisen, M.B., van de Rijn, M., Jeffrey, S.S., Rees, C.A., Pollack, J.R., Ross, D.T., Johnsen, H., Akslen, L.A., et al. (2000). Molecular portraits of human breast tumours. *Nature* 406, 747–752.
- Polyak, K. (2011). Heterogeneity in breast cancer. *J. Clin. Invest.* 121, 3786–3788.
- Roesch, A., Vultur, A., Bogeski, I., Wang, H., Zimmermann, K.M., Speicher, D., Körbel, C., Laschke, M.W., Gimotty, P.A., Philipp, S.E., et al. (2013). Overcoming intrinsic multidrug resistance in melanoma by blocking the mitochondrial respiratory chain of slow-cycling JARID1B(high) cells. *Cancer Cell* 23, 811–825.
- Sakai, W., Swisher, E.M., Karlan, B.Y., Agarwal, M.K., Higgins, J., Friedman, C., Villegas, E., Jacquemont, C., Farrugia, D.J., Couch, F.J., et al. (2008). Secondary mutations as a mechanism of cisplatin resistance in BRCA2-mutated cancers. *Nature* 451, 1116–1120.
- Schiffer, L.M., Braunschweiger, P.G., Stragand, J.J., and Poulakos, L. (1979). The cell kinetics of human mammary cancers. *Cancer* 43, 1707–1719.
- Sharma, S.V., Lee, D.Y., Li, B., Quinlan, M.P., Takahashi, F., Maheswaran, S., McDermott, U., Azizian, N., Zou, L., Fischbach, M.A., et al. (2010). A chromatin-mediated reversible drug-tolerant state in cancer cell subpopulations. *Cell* 141, 69–80.
- Shipitsin, M., Campbell, L.L., Argani, P., Weremowicz, S., Bloushtain-Qimron, N., Yao, J., Nikolskaya, T., Serebryiskaya, T., Beroukhim, R., Hu, M., et al. (2007). Molecular definition of breast tumor heterogeneity. *Cancer Cell* 11, 259–273.
- Silver, D.P., Richardson, A.L., Eklund, A.C., Wang, Z.C., Szallasi, Z., Li, Q., Juul, N., Leong, C.O., Calogrias, D., Buraimoh, A., et al. (2010). Efficacy of neoadjuvant Cisplatin in triple-negative breast cancer. *J. Clin. Oncol.* 28, 1145–1153.

- Stephens, P.J., Tarpey, P.S., Davies, H., Van Loo, P., Greenman, C., Wedge, D.C., Nik-Zainal, S., Martin, S., Varela, I., Bignell, G.R., et al.; Oslo Breast Cancer Consortium (OSBREAC) (2012). The landscape of cancer genes and mutational processes in breast cancer. *Nature* **486**, 400–404.
- Turner, N.C., and Reis-Filho, J.S. (2012). Genetic heterogeneity and cancer drug resistance. *Lancet Oncol.* **13**, e178–e185.
- van de Ven, S., Smit, V.T., Dekker, T.J., Nortier, J.W., and Kroep, J.R. (2011). Discordances in ER, PR and HER2 receptors after neoadjuvant chemotherapy in breast cancer. *Cancer Treat. Rev.* **37**, 422–430.
- Yap, T.A., Gerlinger, M., Futreal, P.A., Pusztai, L., and Swanton, C. (2012). Intratumor heterogeneity: seeing the wood for the trees. *Sci. Transl. Med.* **4**, 127ps110.